Journal of the Korean Crystal Growth and Crystal Technology
Vol. 16, No. 4 (2006) 149-156

Effect of aspect ratio on solutally buoyancy-driven convection in mercurous chloride (Hg_2Cl_2) crystal growth processes

Geug-Tae Kim† and Kyoung-Hwan Lee*

Department of Nano-Bio Chemical Engineering, Hannam University, Taejon 306-791, Korea
**Energy Conversion Research Department, Korea Institute of Energy Research, Taejon 305-343, Korea*

(Received July 24, 2006)
(Accepted August 4, 2006)

Abstract For an aspect ratio (transport length-to-width) of 5, Pr = 2.89, Le = 0.018, Pe = 2.29, Cv = 1.11, P_B = 40 Torr, solutally buoyancy-driven convection ($Gr_s = 3.03 \times 10^5$) due to the disparity in the molecular weights of the component A (Hg_2Cl_2) and B (He) is stronger than thermally buoyancy-driven convection ($Gr_t = 1.66 \times 10^4$). The crystal growth rate is decreased exponentially for $2.5 \leq Ar \leq 5$, with (1) the linear temperature profile and a fixed temperature difference, (2) the imposed thermal profile, a fixed crystal region and varied temperature difference. This is related to the finding that the effects of side walls tend to stabilize convection in the growth reactor. But, with the imposed thermal profile, a fixed source region and varied temperature difference, the rate is increased for $2 \leq Ar \leq 3$, and remains nearly unchanged for $3 \leq Ar \leq 5$.

Key words Mercurous chloride, Solutally buoyancy-driven convection, Aspect ratio, Physical vapor transport

1. Introduction

Interest in growing mercurous chloride (Hg_2Cl_2) single crystal stems from their exceptional optical broad transmission range from 0.36 to 20 μm for applications in acousto-optic and opto-electronic devices such as Bragg cells, X-ray detectors operating at ambient temperature [1]. The equimolar Hg_2Cl_2 compound decomposes to two liquids at a temperature near 525°C where the vapor pressure is well above 20 atm [2, 3]. Because of this decomposition and high vapor pressure, Hg_2Cl_2 cannot be solidified as a single crystal directly from the stoichiometric melt. However, very similar to the mercurous bromide, mercurous chloride exhibits sufficiently high vapor pressure at low temperatures so that these crystals are usually grown by the physical vapor transport (PVT) in closed silica glass ampoules. The PVT processing has many advantages over melt-growth methods since it can be conducted at low temperatures: (1) vapor-solid interfaces possess relatively high interfacial morphological stability against non-uniformities in heat and mass transfer; (2) high purity crystals are achieved; (3) materials decomposed before melting, such as Hg_2Cl_2 can be grown; (4) lower point defect and dislocation densities are achieved [4]. The mechanism of the PVT process is simple: sublimation-condensation in closed silica glass ampoules in temperature gradient imposed between the source material and the growing crystal. In the actual PVT system of Hg_2Cl_2, the molecular species Hg_2Cl_2 sublimes as the vapor phase from the crystalline source material (Hg_2Cl_2), and is subsequently transported and re-incorporated into the single crystalline phase (Hg_2Cl_2) [5]. Recently PVT has become an important crystal growth process for a variety of acousto-optic materials. However, the industrial applications of the PVT process remain limited. One of important main reasons is that transport phenomena occurring in the vapor are complex and coupled so that it is difficult to design or control the process accurately. Such complexity and coupling are associated with the inevitable occurrence of thermal and/or solutal convection generated by the interaction of gravity with density gradients arising from temperature and/or concentration gradients. In general, convection has been regarded as detrimental and, thus, to be avoided or minimized in PVT growth system. These thermal/andor soultal convection-induced complications result in problems ranging from crystal inhomogeneity to structural imperfection. Therefore, in order to analyze and control the PVT process accurately, and also make significant improvements in the process, it is essential to investigate the roles of convection in the PVT process.

Markham, Greenwell and Rosenberger [6] examined the effects of thermal and thermosolutal convections during the PVT process inside vertical cylindrical enclosures for a time-independent system, and showed that

†Corresponding author
Tel: +82-42-629-7984
Fax: +82-42-623-9489
E-mail: gtkim@hannam.ac.kr

even in the absence of gravity, convection can be present, causing nonuniform concentration gradients. They emphasized the role of geometry in the analysis of the effects of convection. As such these fundamentally constitute steady state two-dimensional models. The steady state models are limited to low Rayleigh number applications, because as the Rayleigh number increases oscillation of the flow field occurs. To address the issue of unsteady flows in PVT, Duval [7] performed a numerical study on transient thermal convection in the PVT processing of Hg_2Cl_2 very similar to the mercurous bromide for a vertical rectangular enclosure with insulated temperature boundary conditions for Rayleigh numbers up to 10^6. Nadarajah *et al.* [8] addressed the effects of solutal convection for any significant disparity in the molecular weights of the crystal components and the inert gas. Zhou *et al.* [9] reported that the traditional approach of calculating the mass flux assuming one-dimensional flow for low vapor pressure systems is indeed correct. Rosenberger *et al.* [10] studied three-dimensional numerical modeling of the PVT yielded quantitative agreement with measured transport rates of iodine through octofluorocyclobutane (C_4F_8) as inert background gas in horizontal cylindrical ampoules.

In this theoretical study, a two-dimensional model is used for the analysis of the PVT processes during vapor-growth of mercurous chloride crystals (Hg_2Cl_2) in horizontally oriented, cylindrical, closed ampoules in a two-zone furnace system. Diffusion-limited processes are considered in this paper, although the recent paper of Singh, Mazelsky and Glicksman [11] demonstrated that the interface kinetics plays an important role in the PVT system of Hg_2Cl_2. Solutally buoyancy-driven convection will be considered at this point, primarily for a mixture of Hg_2Cl_2 vapor and impurity of Helium (He). Thermal convection is negligible in comparison to solutally-induced convection for an imposed nonlinear thermal profile to prevent supersaturation along the transport path.

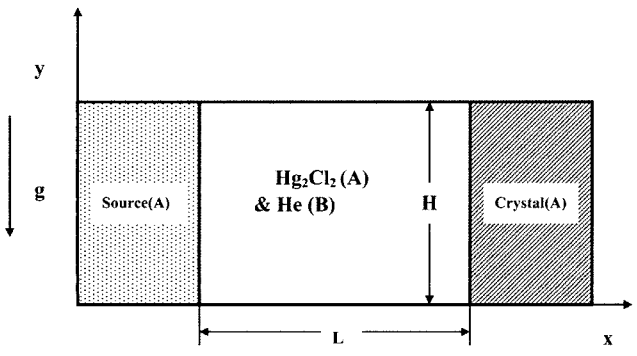

Fig. 1. Schematic of PVT growth reactor in a two-dimensional rectangular system.

It is the purpose of this paper to relate applied solutally buoyancy-driven convection process parameters such as thermal wall profiles, temperature differences between the source and crystal region, aspect ratio (transport length -to-width) to the crystal growth rate and the maximum velocity magnitude to examine the effects of aspect ratio on solutally buoyancy-driven convection in order to gain insights into the underlying physicochemical processes.

2. Physical and Mathematical Formulations

Consider a rectangular enclosure of height H and transport length L, shown in Fig. 1. The source is maintained at a temperature T_s, while the growing crystal is at a temperature T_c, with $T_s > T_c$. PVT of the transported component A (Hg_2Cl_2) occurs inevitably, due to presence of impurities, with the presence of a component B (He). The interfaces are assumed to be flat for simplicity. The finite normal velocities at the interfaces can be expressed by Stefan flow deduced from the one-dimensional diffusion-limited model [12], which would provide the coupling between the fluid dynamics and species calculations. On the other hand, the tangential component of the mass average velocity of the vapor at the interfaces vanishes. Thermodynamic equilibria are assumed at the interfaces so that the mass fractions at the interfaces are kept constant at $\omega_{A,s}$ and $\omega_{A,c}$. On the vertical non-reacting walls appropriate velocity boundary conditions are no-slip, the normal concentration gradients are zero, and wall temperatures are imposed as nonlinear temperature gradients.

Thermophysical properties of the fluid are assumed to be constant, except for the density. When the Boussinesq approximation is invoked, density is assumed constant except the buoyancy body force term. The density is assumed to be a function of both temperature and concentration. The ideal gas law and Dalton's law of partial pressures are used. Viscous energy dissipation and the Soret-Dufour (thermo-diffusion) effects can be neglected, as their contributions remain relatively insignificant for the conditions encountered in our PVT crystal growth processes. Radiative heat transfer can be neglected under our conditions, based on Kassemi and Duval [13].

The transport of fluid within a rectangular PVT crystal growth reactor is governed by a system of elliptic,

coupled conservation equations for mass (continuity), momentum, energy and species (diffusion) with their appropriate boundary conditions. Let v_x, v_y denote the velocity components along the x- and y-coordinates in the x, y rectangular coordinate, and let T, ω_A, p denote the temperature, mass fraction of species A (Hg_2Cl_2) and pressure, respectively.

The dimensionless variables are scaled as follows:

$$x^* = \frac{x}{H},\ y^* = \frac{y}{H}, \tag{1}$$

$$u = \frac{u_x}{U_c},\ v = \frac{v_y}{U_c},\ p = \frac{p}{\rho_c U_c^2}, \tag{2}$$

$$T^* = \frac{T-T_c}{T_s-T_c},\ \omega_A^* = \frac{\omega_A-\omega_{A,c}}{\omega_{A,s}-\omega_{A,c}}. \tag{3}$$

The dimensionless governing equations are given by:

$$\nabla^* \bullet V^* = 0, \tag{4}$$

$$\vec{V}^* \bullet \nabla^* \vec{V}^* = -\nabla^* p^* + Pr\nabla^{*2}\vec{V}^* - Ra \cdot Pr \cdot T^* \cdot e_g, \tag{5}$$

$$\vec{V}^* \bullet \nabla^* T^* = \nabla^{*2} T^* \tag{6}$$

$$\vec{V}^* \bullet \nabla^* \omega_A^* = \frac{1}{Le}\nabla^{*2}\omega_A^* \tag{7}$$

These nonlinear, coupled sets of equations are numerically integrated with the following boundary conditions:

On the walls ($0 < x^* < L/H$, $y^* = 0$ and 1):

$$u(x^*, 0) = u(x^*, 1) = v(x^*, 0) = v(x^*, 1) = 0 \tag{8}$$

$$\frac{\partial \omega_A^*(x^*,0)}{\partial y^*} = \frac{\partial \omega_A^*(x^*,1)}{\partial y^*} = 0,$$

$$T^*(x^*,0) = T^*(x^*,1) = \frac{T-T_c}{T_s-T_c}$$

On the source ($x^* = 0$, $0 < y^* < 1$):

$$u(0,y^*) = -\frac{1}{Le(1-\omega_{A,s})}\frac{\Delta\omega}{}\frac{\partial \omega_A^*(0,y^*)}{\partial x^*}, \tag{9}$$

$$v(0,y^*) = 0,$$

$$T^*(0,y^*) = 1,$$

$$\omega_A^*(0,y^*) = 1.$$

On the crystal ($x^* = L/H$, $0 < y^* < 1$):

$$u(L/H,y^*) = -\frac{1}{Le(1-\omega_{A,c})}\frac{\Delta\omega}{}\frac{\partial \omega_A^*(L/H,y^*)}{\partial x^*}, \tag{10}$$

$$v(L/H,y^*) = 0,$$

$$T^*(L/H,y^*) = 0,$$

$$\omega_A^*(L/H,y^*) = 0.$$

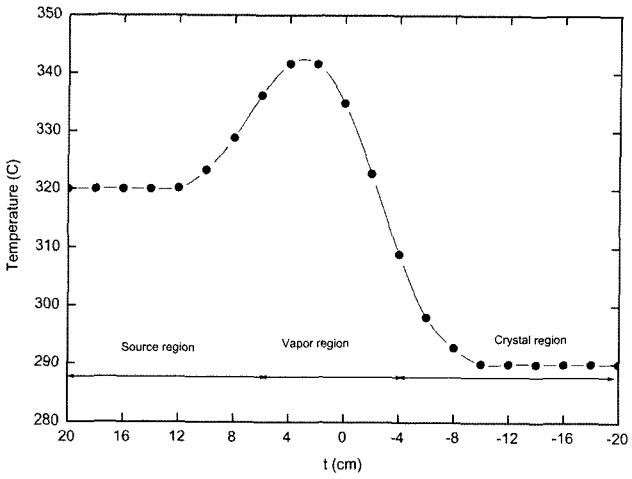

Fig. 2. The temperature profile along the ampoule [14].

The following temperature profile was used as a boundary condition along the ampoule (y = 0 and y = H): this equation is expressed in reference to an approximate fit of experimental data [14, 15], see Fig. 2.

$$T(t) = \begin{cases} 563.16 & \text{for } -20 \le t \le -10 \text{ cm} \\ 608 + 4.97t - 0.70t^2 - 5.91 & \\ \times 10^{-2}t^3 + 6.67\times 10^{-3}t^4 & \\ + 2.60\times 10^{-4}t^5 - 2.49\times 10^{-5}t^6 & \text{for } -10 \le t \le 12 \text{ cm} \\ 593.16 & \text{for } 12 \le t \le 20 \text{ cm} \end{cases} \tag{11}$$

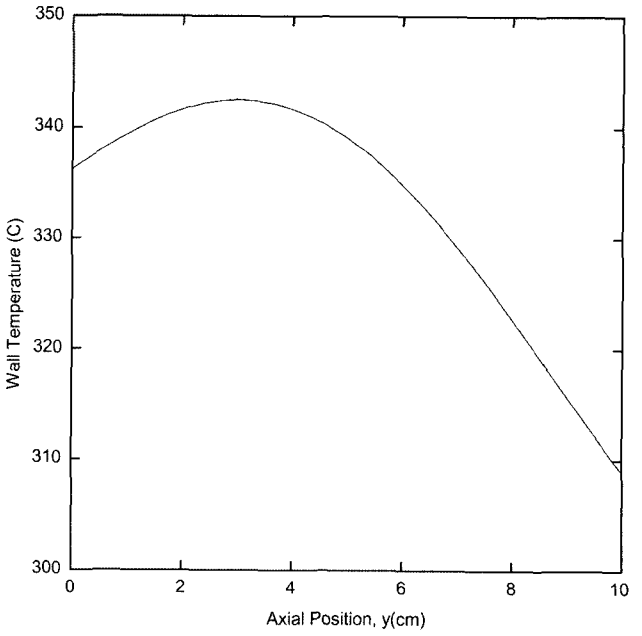

Fig. 3. An axial temperature profile given by Eq. (11) with maximum ("hump") between T_s and T_c.

Relative to Fig. 2, during the crystal growth the ampoule is placed in the nonlinear thermal profile as shown in Fig. 3. The hump region corresponds to the location of the vapor component A and B inside the ampoule. The source material lies in the region with the larger temperature near $t \geq 8$ cm. Whereas crystal growth occurs in the region corresponding to $t \leq -4$ cm. In our experiments one positions the ampoule in the growth region with a temperature less than the source in order to drive the process. In addition, the length of the hump region can also be adjusted so that we have a much larger source region. With respect to Fig. 3, the following transformation is used to relate the laboratory reference to the ampoule: where K_i is the position of the source and vapor interface in the laboratory reference frame.

$$x = K_i - t$$

In the dimensionless parameters in the governing equations the thermophysical properties of the gas mixture are estimated from gas kinetic theory using Chapman-Enskog's formulas [16].

The vapor pressure [17] p_A of Hg_2Cl_2 (in the unit of Pascal) can be evaluated from the

$$p_A = e^{(a - b/T)} \tag{12}$$

following formula as a function of temperature: in which a = 29.75, b = 11767.1.

The crystal growth rate V_c is calculated from a mass balance at the crystal vapor interface, assuming fast kinetics, i.e. all the vapor is incorporated into the crystal, which is given by (subscripts c, v refer to crystal and vapor respectively)

$$\int \rho_v u_v \cdot n dA = \int \rho_c u_c \cdot n dA, \tag{13}$$

$$u_c = \frac{\rho_v \int u_v \cdot n dA}{\rho_c \int dA}. \tag{14}$$

The detailed numerical schemes in order to solve the discretization equations for the system of nonlinear, coupled governing partial differential equations are found in [18].

3. Results and Discussion

One of the purposes for this study is to correlate the growth rate to process parameters such as an aspect ratio, a nonlinear and a linear thermal profile. Thus, it is desirable to express some results in terms of dimensional growth rate, however they are also applicable to parameter ranges over which the process varies in the manner given. The six dimensionless parameters, namely Gr, Ar, Pr, Le, C_v and Pe, are independent and arise naturally from the dimensionless governing equations and boundary conditions. The dimensionless parameters and physical properties for the operating conditions of this study are shown in Table 1.

Table 1
Typical thermo-physical properties used in this study (M_A = 472.086, M_B = 4.003)

Transport length, L	10 cm
Height, H	2 cm
Source temperature, T_s	336.21°C
Crystal temperature, T_c	308.89°C
Density, ρ	0.0019 g/cm^3
Dynamic viscosity, μ	0.00028 g/(cm•sec)
Diffusivity, D_{AB}	2.80 cm^2/s
Thermal expansion coefficient, β	0.0017 K^{-1}
Prandtl number, Pr	2.89
Lewis number, Le	0.018
Peclet, Pe	2.29
Concentration number, Cv	1.11
Total system pressure, P_T	164.65 Torr
Partial pressure of component B, P_B	40 Torr
Thermal Grashof number, Gr_t	1.66×10^4
Solutal Grashof number, Gr_s	3.03×10^5

When the molecular weight of a light element (He) is not equal to that of the crystal component (Hg_2Cl_2) during the physical vapor transport, both solutal and thermal effects should be considered. If solutal convection is dominant, the imposed temperature profile has little effect on the growth rate [8]. Conductive wall boundary conditions with both a nonlinear and a linear thermal profile are considered, while the insulated walls are not considered because it is difficult to obtain in practice and most of vapor growth experiments are performed under the imposed nonlinear thermal profile to avoid nucleation at the ampoule walls. Figure 3 shows the axial temperature profile given by Eq. (11) with maximum ("hump") between T_s and T_c. To prevent undesirable nucleations at the walls, an often used experimental technique is to impose a nonlinear thermal profile with a maximum between the crystal and the source, and is usually referred to as a temperature "hump". This temperature hump could eliminate the problem of vapor supersaturation along the transport path and, thus, of parasitic nucleations at the walls. But, these humps may result in sharp temperature gradients near the crystal region, inducing thermal stresses and a decrease in crystal quality. A temperature hump of 27 K with T_s =

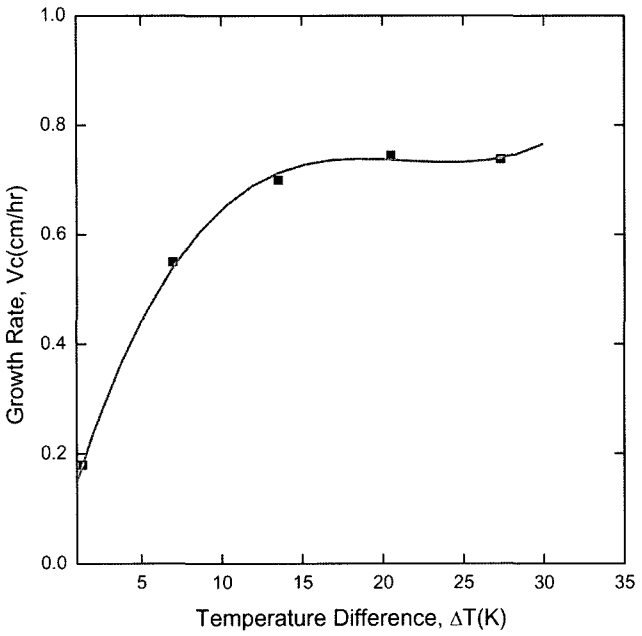

Fig. 4. Growth rates of Hg_2Cl_2 as a function of the temperature difference between the source and the crystal region, ΔT(K), for 1 K ≤ ΔT ≤ 30 K.

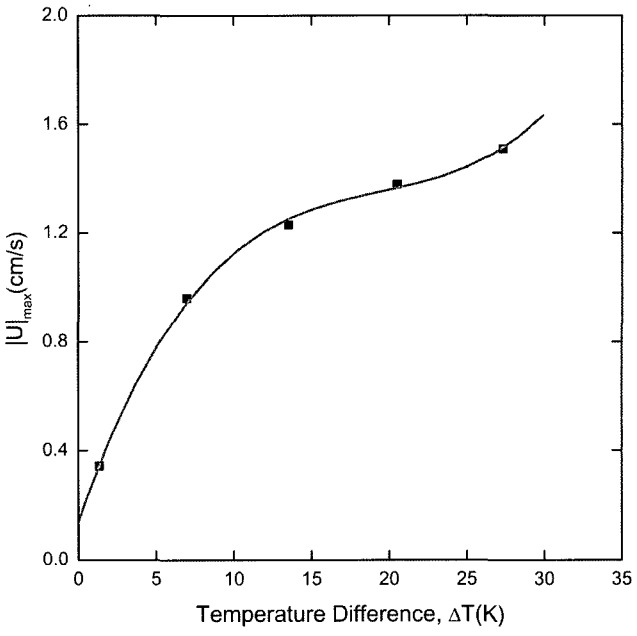

Fig. 5. The $|U|_{max}$ as a function of the temperature difference between the source and the crystal region, ΔT(K), corresponding to Fig. 4.

336°C, T_c = 309°C is typically selected for this study.

Figure 4 shows the growth rates of Hg_2Cl_2 as a function of the temperature difference between the source and the crystal region, ΔT (K), for 1 K ≤ ΔT ≤ 30 K, with a nonlinear thermal profile. With a linear temperature profile, the vapor of component A (Hg_2Cl_2) is in a supersaturation throughout the ampoule [19]. It is clear to see why a linear temperature profile is rarely used in practice [8, 19]. For 1 K ≤ ΔT ≤ 15 K, the growth rate is increased approximately by a factor of 3. For 15 K ≤ ΔT ≤ 30 K, the rate is nearly invariant, which might be due to the role of kinetic effects on the crystal region and/or the effects of side walls. Figure 5 corresponds to the Fig. 4. As shown in Fig. 5, with increasing the temperature difference, ΔT, the maximum magnitude of velocity vector which means the intensity of convection flows sharply increases for 1 K ≤ ΔT ≤ 15 K, and slightly increases for 15 K ≤ ΔT ≤ 30 K. In other words, for the temperature differences below 15 K, the convective intensity is sensitive to the temperature difference compared to the ranges of from 15 K up to 30 K. The former has a gradient of 0.073 cm/s•K, while the latter has a gradient of 0.02 cm/s•K. It reflects the importance of solutal convection compared to thermal convection. Figures 4 and 5 are based on ΔT = 27.32 K are Ar = 5, Pr = 2.89, Le = 0.018, Pe = 2.29, Cv = 1.11, Gr_t (thermal Grashof number) = 1.66 × 10^4, Grs (solutal Grashof number) = 3.03 × 10^5, P_B = 40 Torr. The intensity of solutal convection is greater than that of thermal convection by one order of magnitude.

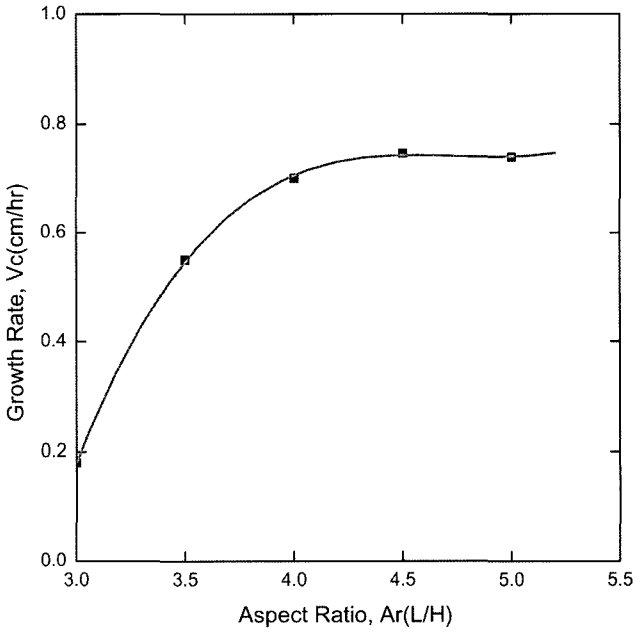

Fig. 6. Effects of aspect ratio Ar (L/H) on the crystal growth rates of Hg_2Cl_2, with the source region of the position fixed.

Figure 6 shows the effects of aspect ratio, Ar (L/H) on the crystal growth rates of of Hg_2Cl_2, with the source region of the position fixed. For 3 ≤ Ar ≤ 4, the rate is sharply increased with increasing the aspect ratio, while for 4 ≤ Ar ≤ 5, the rate remains nearly invariant, which indicates the role of kinetic effects on the crystal region

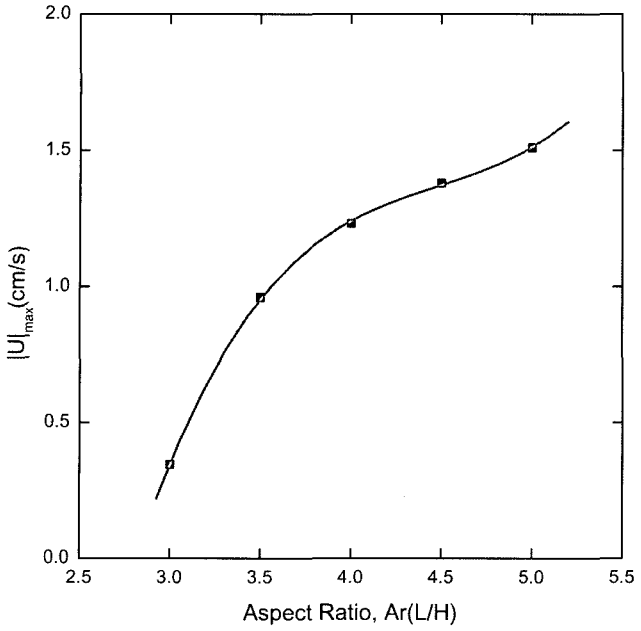

Fig. 7. The $|U|_{max}$ as a function of the aspect ratio Ar (L/H), corresponding to Fig. 6.

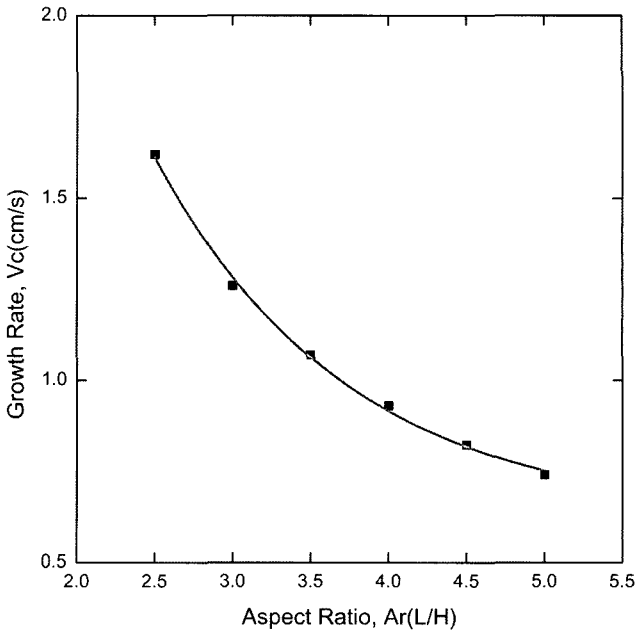

Fig. 8. Effects of aspect ratio Ar (L/H) on the crystal growth rates of Hg_2Cl_2, with the linear thermal profiles, i.e., conducting walls for ΔT = 27.32 K, Pr = 2.89, Le = 0.018, Pe = 2.29, Cv = 1.11, Gr_t (thermal Grashof number) = 1.66×10^4, Gr_s (solutal Grashof number) = 3.03×10^5, P_B = 40 Torr.

as well as the effects of side wall. The effects of side walls tend to stabilize convection in the growth reactor. This tendency is consistent with the results [20] on the pure thermal convection without crystal growth in enclosures. Considering Figs. 4 and 5, the side walls influence more significantly on the rate than thermal convective effects. Note that Figs. 4 through 7 are based on the fixed source region, which results in changing the aspect ratio through moving the crystal region. Figure 7 corresponds to Fig. 6. As shown in Fig. 7, the maximum velocity magnitudes versus the aspect ratios show the same trend as that versus the temperature difference shown in Fig. 5. In actual crystal growth system, the temperature profile is intimately related to the aspect ratio because the temperature profile is so imposed that it could not be altered. In particular, for the temperature differences under considerations in this study, the aspect ratio is directly proportional to the temperature difference, with a fixed source region.

One now investigates the effects of the side walls on the growth rate and the maximum velocity magnitude of convective flow. Figure 8 illustrates the effects of aspect ratio on the rate, with the linear thermal profile, i.e., conducting walls for ΔT = 27.32 K, Pr = 2.89, Le = 0.018, Pe = 2.29, Cv = 1.11, Gr_t (thermal Grashof number) = 1.66×10^4, Gr_s (solutal Grashof number) = 3.03×10^5. As the aspect ratio increases from 2.5 up to 5.0, the rate decays exponentially. As pointed out before, this is not surprising that the effects of side walls tend to

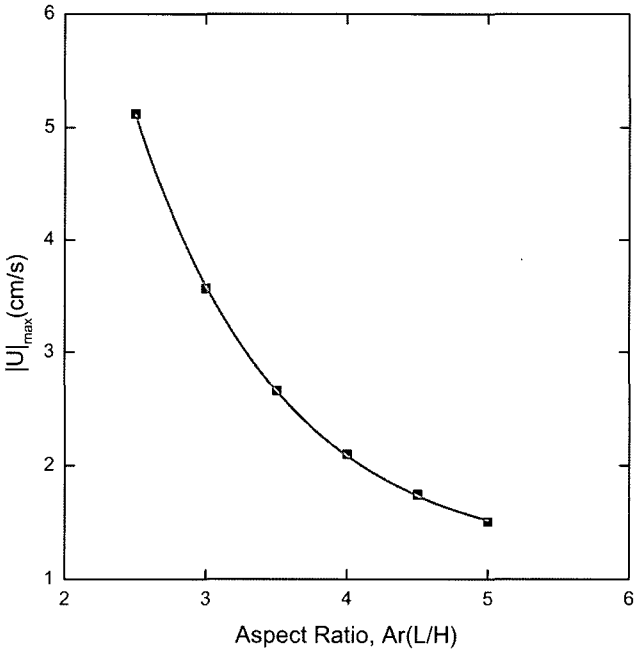

Fig. 9. The $|U|_{max}$ as a function of the aspect ratio Ar (L/H), corresponding to Fig. 8.

stabilize convection in the growth reactor. Figure 9 corresponds to Fig. 8. Figure 9 shows the maximum magnitude of velocity vector, |U|max as a function of aspect ratio. The maximum magnitude decreases exponentially with increasing the aspect ratio from 2.5 to 5. For the ranges below Ar = 3, the rate and the maximum magni-

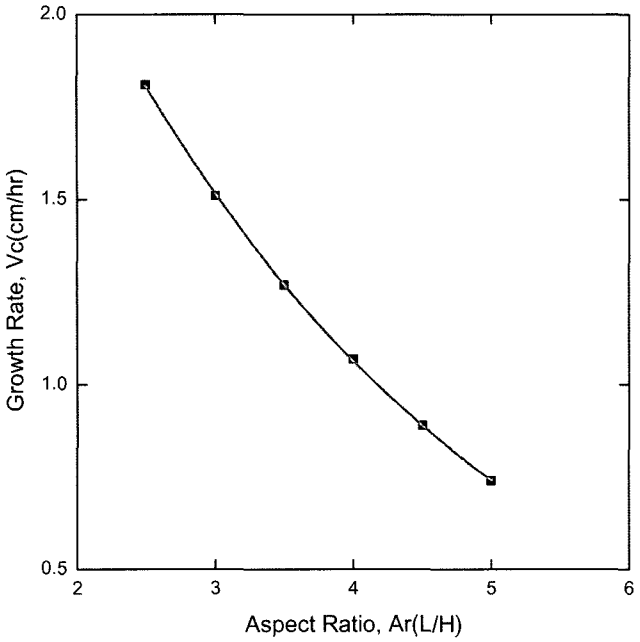

Fig. 10. Growth rates of Hg_2Cl_2 as a function of the aspect ratio Ar (L/H), with the crystal region of the position which is fixed, for 27 K ≤ ΔT ≤ 35 K.

tude are sharply decreased because of the effects of side walls. It should be noted that the temperature difference between the source and crystal region is fixed, i.e., ΔT = 27.32 K. Figure 10 shows the rate of Hg_2Cl_2 as a function of the aspect ratio Ar, with a fixed crystal region, and a nonlinear thermal profile. The aspect ratios of 2.5 through 5 are considered here with their corresponding temperature ranges, 27 K ≤ ΔT ≤ 35 K. Unlike in the cases of the fixed source region and nonlinear thermal profile (Figs. 4 and 6), the effects of side walls are shown to be significant in the cases of the fixed crystal region and nonlinear thermal profile (Figs. 10 and 11). As shown in Fig. 10, the rate is decreased exponentially for 2.5 ≤ Ar ≤ 5. Figure 11 illustrates the rate of Hg_2Cl_2 as a function of the temperature difference. The rate is linearly proportional to the temperature difference. For the cases of Ar = 2.5 and 3, the rates deviates greatly from the trend line, which is not clear at present. This might be a coupling of temperature difference and aspect ratio which is related to the nonlinear thermal profile imposed in the actual crystal system and adjustment of the aspect ratio. For the aspect ratios lower than 3, the growth rate is more significantly influenced by aspect ratio than by the temperature difference. The rates for the aspect ratios lower than 3 is considerably greater than for the ratios of 3 above, which indicates the effects of side walls.

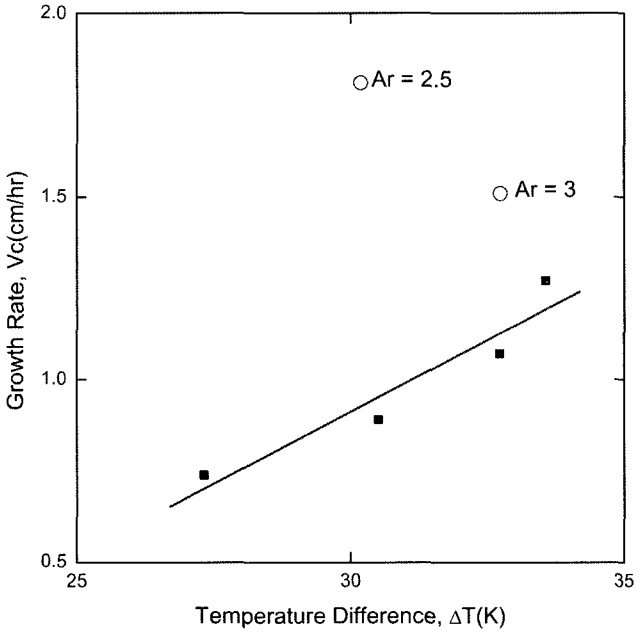

Fig. 11. Growth rates of Hg_2Cl_2 as a a function of the temperature difference between the source and the crystal region, ΔT(K), for 27 K ≤ ΔT ≤ 35 K and 2.5 ≤ Ar ≤ 5, which corresponds to Fig. 10. The crystal region of the position is fixed.

4. Conclusions

It is concluded that the solutally buoyancy-driven convection (Gr_s = 3.03 × 10^5) due to the disparity in the molecular weights of the component A (Hg_2Cl_2) and B (He) is stronger than thermally buoyancy-driven convection (Gr_t = 1.66 × 10^4), for an aspect ratio (transport length-to-width) of 5, Pr = 2.89, Le = 0.018, Pe = 2.29, Cv = 1.11, P_B = 40 Torr. The rate is decreased exponentially for 2.5 ≤ Ar ≤ 5, with (1) the linear temperature profile and a fixed temperature difference, and (2) the imposed thermal profile, a fixed crystal region and varied temperature differences. This is related to the findings that the effects of side walls tend to stabilize convection in the growth reactor. But, with the imposed thermal profile, a fixed source region and varied temperature differences, the rate is increased for 2 ≤ Ar ≤ 3, and remains nearly unchanged for 3 ≤ Ar ≤ 5. It is likely to be due to a coupling of the effects of side walls and kinetics across the crystal region. At this point, a clear explanation on these phenomena remains further study. The findings were reported in ref. [11].

Acknowledgements

The authors wish to appreciate the financial support

provided by the Hannam University through the Kyobi program of research project number of 2005A064 (April 1, 2005 through March 31, 2006).

References

[1] N.B. Singh, M. Gottlieb, G.B. Brandt, A.M. Stewart, R. Mazelsky and M.E. Glicksman, "Growth and characterization of mercurous halide crystals:mercurous bromide system", J. Crystal Growth 137 (1994) 155.

[2] N.B. Singh, R.H. Hopkins, R. Mazelsky and J.J. Conroy, "Purification and growth of mercurous chloride single crystals", J. Crystal Growth 75 (1970) 173.

[3] S.J. Yosim and S.W. Mayer, "The mercury-mercuric chloride system", J. Phys. Chem. 60 (1960) 909.

[4] F. Rosenberger, "Fluid dynamics in crystal growth from vapors", Physico-Chemical Hydro-dynamics 1 (1980).

[5] N.B. Singh, M. Gottlieb, A.P. Goutzoulis, R.H. Hopkins and R. Mazelsky, "Mercurous Bromide acousto-optic devices", J. Crystal Growth 89 (1988) 527.

[6] B.L. Markham, D.W. Greenwell and F. Rosenberger, "Numerical modeling of diffusive-convective physical vapor transport in cylindrical vertical ampoules", J. Crystal Growth 51 (1981) 426.

[7] W.M.B. Duval, "Convection in the physical vapor transport process-- I: Thermal", J. Chemical Vapor Deposition 2 (1994) 188.

[8] A. Nadarajah, F. Rosenberger and J. Alexander, "Effects of buoyancy-driven flow and thermal boundary conditions on physical vapor transport", J. Crystal Growth 118 (1992) 49.

[9] H. Zhou, A. Zebib, S. Trivedi and W.M.B. Duval, "Physical vapor transport of zinc-telluride by dissociative sublimation", J. Crystal Growth 167 (1996) 534.

[10] F. Rosenberger, J. Ouazzani, I. Viohl and N. Buchan, "Physical vapor transport revised", J. Crystal Growth 171 (1997) 270.

[11] N.B. Singh, R. Mazelsky and M.E. Glicksman, "Evaluation of transport conditions during PVT: mercurous chloride system", PhysicoChemical Hydrodynamics 11 (1989) 41.

[12] F. Rosenberger and G. Müller, "Interfacial transport in crystal growth, a parameter comparison of convective effects", J. Crystal Growth 65 (1983) 91.

[13] M. Kassemi and W.M.B. Duval, "Interaction of surface radiation with convection in crystal growth by physical vapor transport", J. Thermophys. Heat Transfer 4 (1989) 454.

[14] N.B. Singh and W.M. B. Duval, "Growth kinetics of physical vapor transport processes: crystal growth of the optoelectronic material mercurous chloride", NASA Technical Memorandum 103788 (1991).

[15] C. Mennetrier, W.M.B. Duval, and N.B. Singh, "Physical vapor transport of mercurous chloride under a nonlinear thermal profile", NASA Technical Memorandum 105920 (1992).

[16] R.B. Bird, W.E. Stewart and E.N. Lightfoot, *Transport Phenomena* (New York, NY: John Wiley and Sons, 1960).

[17] C. Mennetrier and W.M.B. Duval, "Thermal-solutal convection with conduction effects inside a rectangular enclosure", NASA Technical Memorandum 105371 (1991).

[18] S.V. Patankar, Numerical Heat Transfer and Fluid Flow, (Washington D. C.: Hemisphere Publishing Corp., 1980).

[19] G.T. Kim, "Convective-diffusive transport in mercurous chloride (Hg_2Cl_2) crystal growth", J. Ceramic Processing Research 6(2005) 110.

[20] I. Catton, "Effect of wall conducting on the stability of a fluid in a rectangular region heated from below", J. Heat Transfer 94 (1972) 446.